# Expected ON–minus–OFF deflections with matched OFF positions for calibrator sources at 151, 235, 325, 610 and 1420 MHz

Dharam Vir Lal, Ishwara-Chandra C.H. and Jayprakash R. Kamble
dharam/ishwar/jprakash AT ncra DOT tifr DOT res DOT in

November 3, 2015

## Contents



## List of Figures



## List of Tables

**Abstract**

In this report, we provide (i) $T_{\rm sky}$ measurements towards Cas A, Crab, Cygnus A and Virgo A, henceforth called as $T_{\rm ON}$, and (ii) several locations around these calibration sources with matched background $T_{\rm sky}$ which we call as $T_{\rm OFF}$ for regular ON–minus–OFF measurements as part of the Post-Maintenance-Quality-Tests. Using these measurements we provide expected amount of deflection, ON–minus–OFF in dB for each of these calibrator sources. The key inputs in order to generate Table 4 are Table 1, 3 and 5; or more specifically, $T_{\rm sky}$ values listed in Section 2 of absolute cold sky brightness temperature of the diffuse radio background from 50 MHz to 1500 MHz (Lal 2014), and flux density measurements for Cas A, Crab, Cygnus A & Virgo A calibrator sources from 50 to 1450 MHz (Lal 2015). We also summarise some salient features of this document, its superiority over currently used OFF position co-ordinates used currently by the control-room. We hope this document would be useful for our GMRT colleagues from the Engineering group and control-room staff to perform routine system tests and characterise the system.

# 1 Introduction

The on-going upgrade of the GMRT have renewed interest in the measured system temperature at each observing frequency. Since efforts are being made to have lowest possible receiver temperature, hence an absolute value of ON calibration source and OFF source sky temperature are a must in order to determine absolute deflection, head-room below the saturation limits, etc.

In an earlier report, absolute cold sky brightness temperature of the diffuse radio background from 50 to 1500 MHz (Lal 2014), we discussed basics, a small background of radio astronomy, including flux density and intensity, surface brightness, brightness temperature, what does the radio telescope detect, antenna temperature, etc. Here we use these basics and present the methodology, Section 2 and summarise our findings, Section 3.

Table 1: $T_{\rm sky}$ at 408 MHz for calibrator sources. We list the ON and OFF $T_{\rm sky}$ measurements and their J2000 coordinates.

| | | $Gal_{Lon}$ (degree) | $Gal_{Lat}$ (degree) | R.A. (J2000) (hh mm ss.ss) | Dec (J2000) (dd mm ss.s) | $T_{\rm sky}$ (K) |
|---|---|---|---|---|---|---|
| Cygnus A | | | | | | |
| | ON | 76.113 | 5.801 | 19 59 03.47 | +40 41 31.5 | 2993.0 |
| | OFF–1 | 79.277 | 15.645 | 19 18 05.89 | +47 59 23.8 | 41.1 |
| | OFF–2 | 62.402 | 10.723 | 19 06 06.33 | +31 00 00.9 | 41.4 |
| Cas A | | | | | | |
| | ON | 111.621 | −2.285 | 23 22 58.52 | +58 37 49.8 | 3432.0 |
| | OFF–1 | 99.316 | −4.395 | 22 13 29.43 | +51 05 16.9 | 45.1 |
| | OFF–2 | 121.113 | −5.801 | 00 38 08.03 | +57 01 25.5 | 47.6 |
| Crab | | | | | | |
| | ON | −175.605 | −5.801 | 05 34 05.88 | +22 08 31.4 | 317.0 |
| | OFF–1 | −164.355 | −6.152 | 05 56 56.42 | +12 21 40.9 | 38.7 |
| | OFF–2 | 164.004 | −7.910 | 04 29 43.30 | +36 59 59.3 | 38.2 |
| Virgo A | | | | | | |
| | ON | −76.113 | 74.004 | 12 30 20.75 | +11 55 02.1 | 230.7 |
| | OFF–1 | −85.605 | 70.488 | 12 14 10.41 | +09 42 34.0 | 16.4 |
| | OFF–2 | −75.762 | 80.332 | 12 38 27.89 | +17 56 04.1 | 18.4 |

Table 2: System parameters listed in GMRT observer's manual, and sky temeperatures, $T_{\rm sky}$ as extrapolated to several GMRT frequencies from 408 MHz temperature map (Sirothia 2009, Haslam 1981, 1982).

| | | Frequency (MHz) | | | |
|---|---|---|---|---|---|
| | 151 | 235 | 325 | 610 | 1420 |
| Antenna Gain (K Jy$^{-1}$ Antenna)$^{-1}$ | 0.33 | 0.33 | 0.32 | 0.32 | 0.22 |
| Receiver Temperature, $T_{\rm Rx}$ (K) | 295$^{\dagger}$ | 106$^{\dagger}$ | 53 | 60 | 45 |
| Typical $\rm T_{ground}$ (K) | 12 | 32 | 13 | 32 | 24 |
| $T_{\rm sky}$ (Cygnus A) | | | | | |
| OFF-1 (K) | 518.4 | 167.8 | 73.4 | 14.7 | 1.7 |
| OFF-2 (K) | 522.1 | 169.0 | 73.9 | 14.8 | 1.7 |
| $T_{\rm sky}$ (Cas A) | | | | | |
| OFF-1 (K) | 568.8 | 184.1 | 80.5 | 16.2 | 1.9 |
| OFF-2 (K) | 600.3 | 194.3 | 85.0 | 17.1 | 2.0 |
| $T_{\rm sky}$ (Crab) | | | | | |
| OFF-1 (K) | 488.1 | 158.0 | 69.1 | 13.9 | 1.6 |
| OFF-2 (K) | 481.8 | 156.0 | 68.2 | 13.7 | 1.6 |
| $T_{\rm sky}$ (Virgo A) | | | | | |
| OFF-1 (K) | 206.8 | 67.0 | 29.3 | 5.9 | 0.7 |
| OFF-2 (K) | 232.1 | 75.1 | 32.9 | 6.6 | 0.8 |

## 2 Method

Table 1 gives coordinates for the ON and OFF calibrator sources. Table 3 gives flux densities ($S_\nu$) and ON source temperatures ($T_{\rm ON,\ \nu}$) for the calibrator sources at several GMRT frequencies. We use

$$T^{\rm cal}_{\rm src,\ \nu} = S^{\rm cal}_{\nu} \times G$$

where $G$ is the antenna gain in K Jy$^{-1}$, listed in Tables 2 and 5 to determine ON source temperatures. Next

$$T_{\rm sky} \ \propto \ (1/\nu)^{-\gamma}$$

where $\gamma$ is typically 2.55 (Sirothia 2009) at low frequencies. We use this power-law to determine $T_{\rm sky}$ at other GMRT frequencies, which are tabulated in Table 2.

The total ON source system temperature in the direction of a calibrator at a frequency, $\nu$ is given as

$$T^{\rm cal,Tot}_{\rm ON,\ \nu} \ = \ T^{\rm cal}_{\rm src,\ \nu} + T_{\rm Rx,\ \nu} + T_{\rm grd,\ \nu} + T^{\rm cal}_{\rm sky,\ \nu}$$

and the OFF source system temperature adjacent to the calibrator at a frequency, $\nu$ is given as

$$T^{\rm cal,Tot}_{\rm OFF,\ \nu} \ = \ T^{\rm cal}_{\rm sky,\ \nu} + T_{\rm Rx,\ \nu} + T_{\rm grd,\ \nu} \ .$$

Where, $T_{\rm Rx,\ \nu}$ and $T_{\rm grd,\ \nu}$ are receiver and typical ground temperatures, and $T^{\rm cal}_{\rm src,\ \nu}$ and $T^{\rm cal}_{\rm sky,\ \nu}$ are sky temperatures in the direction of a calibrator and adjacent to the calibrator, respectively at a given frequency. Table 5 lists typical receiver ($T_{\rm Rx}$) and ground ($T_{\rm grd}$) temperatures. The amount of deflection, "ON minus OFF", in dB is then given as

$$10 \log_{10} \left(\frac{T^{\rm cal,Tot}_{\rm ON,\ \nu}}{T^{\rm cal,Tot}_{\rm OFF,\ \nu}}\right) \ .$$

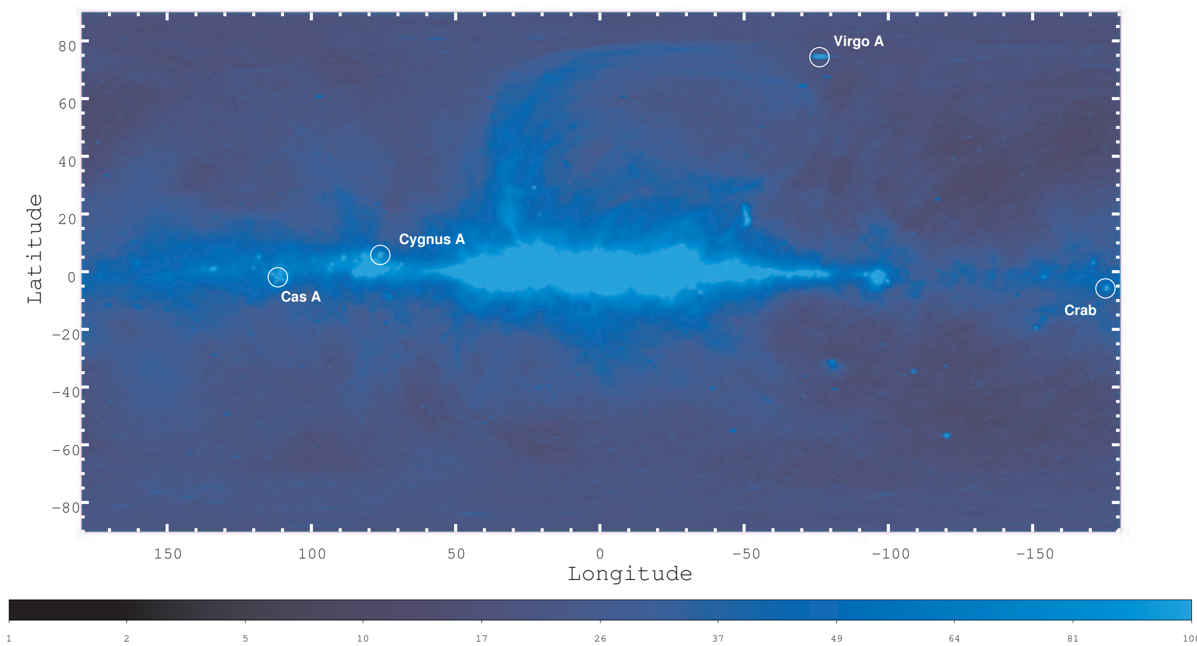


Figure 1: Figure showing all sky temperature image at 408 MHz (Haslam 1981, 1982). Calibrator sources Cygnus A, Cas A, Crab, and Virgo A are labeled. Also shown is the colorbar giving temperature range from 1 K to 100 K.

## 3 Summary of Results

The temperature of the cold sky as a function of observing frequencies of the upgraded GMRT (uGMRT) are tabulated in Table 1 and plotted in Fig. 1 in "absolute cold sky brightness temperature of the diffuse radio background from 50 to 1500 MHz (Lal 2014)". Here, based on methodology described above (Section 2), we present expected deflection (in dB) for ON–minus–OFF measurements for each of these calibrator sources at five GMRT frequencies, namely 151, 235, 325, 610 and 1420 MHz in Table 4 (upper-half). For the sake of completion, assuming that antenna gain $G$, receiver temperature $T_{\rm Rx,\ \nu}$ and ground temperature $T_{\rm grd,\ \nu}$ measurements of the 1420 MHz also holds good for the four sub-bands of the $L$-band, namely 1060, 1170, 1280 and 1390 MHz, we present expected deflection (in dB) for ON–minus–OFF measurements for each of these calibrator sources at these sub-band frequencies in Table 4 (lower-half) as well. In future, once we have $T_{\rm Rx,\ \nu}$ and $T_{\rm grd,\ \nu}$, typical receiver and ground temperature measurements in steps of 5 MHz frequency intervals from 50 MHz to 1500 MHz, we will provide corresponding estimates of the expected deflection for ON–minus–OFF measurements for each of these calibrator sources in steps of 5 MHz frequency intervals. This would then correspond to the frequency coverage of the new feeds of the uGMRT having (nearly) seamless frequency coverage, once the upgrade is complete.

We believe these ON and OFF coordinates should be used for routine ON–minus–OFF measurements as part of system tests by the Engineers. We have also looked at currently used OFF position coordinates, e.g., north-pole or the coordinates provided by R. Athreya & K.S. Jeeva, and suggest that these new OFF position coordinates should be used henceforth, because

1) The new coordinates for the OFF positions are typically $\sim$10 deg away from the coordinates of the calibrator sources, sufficiently away so that the calibrator sources do not appear the side-lobes of the antennas beam in any of the GMRT frequency bands. These OFF positions reside in the same ambient medium, where the calibrator sources reside.

Table 3: Flux densities ($S_\nu$) and ON source temperatures for calibrator sources at several GMRT frequencies. Note the flux density values for each of the calibrator sources at several GMRT frequencies are from "flux density measurements for Cas A, Crab, Cygnus A & Virgo A calibrator sources from 50 to 1450 MHz (Lal 2015)" and the corresponding ON source temperatures are from antenna gain measurements listed in Table 5.

| | Cygnus A | | Cas A | | Crab | | Virgo A | |
|---|---|---|---|---|---|---|---|---|
| | ($S_\nu$) (Jy) | ($T^{\rm cal}_{{\rm src},\ \nu}$) (K) | ($S_\nu$) (Jy) | ($T^{\rm cal}_{{\rm src},\ \nu}$) (K) | ($S_\nu$) (Jy) | ($T^{\rm cal}_{{\rm src},\ \nu}$) (K) | ($S_\nu$) (Jy) | ($T^{\rm cal}_{{\rm src},\ \nu}$) (K) |
| GMRT bands | | | | | | | | |
| 151 MHz | 10141.0 | 3346.5 | 13159.5 | 4342.6 | 1527.5 | 504.1 | 1228.4 | 405.4 |
| 235 MHz | 7190.0 | 2372.7 | 9550.4 | 3151.6 | 1373.2 | 453.2 | 863.9 | 285.1 |
| 325 MHz | 5608.7 | 1794.8 | 7576.7 | 2424.5 | 1271.5 | 406.9 | 670.0 | 214.4 |
| 610 MHz | 3462.6 | 1108.0 | 4833.2 | 1546.6 | 1095.1 | 350.4 | 408.9 | 130.8 |
| 1420 MHz | 1812.6 | 398.8 | 2643.8 | 581.6 | 896.2 | 197.2 | 210.8 | 46.4 |
| Sub-bands of $L$-band | | | | | | | | |
| 1060 MHz | 2267.6 | 498.9 | 3257.6 | 716.7 | 960.6 | 211.3 | 265.2 | 58.3 |
| 1170 MHz | 2102.5 | 462.6 | 3035.8 | 667.9 | 938.4 | 206.4 | 245.4 | 54.0 |
| 1280 MHz | 1962.6 | 431.8 | 2847.2 | 626.3 | 918.6 | 202.1 | 228.7 | 50.3 |
| 1390 MHz | 1842.5 | 405.4 | 2684.4 | 590.6 | 900.8 | 198.2 | 214.4 | 47.2 |

2) Currently used OFF position coordinates:
   (i) For Cygnus A and Crab sources, the OFF position coordinates reside in low temperature region (in 408 MHz map), $\sim$25 K as compared to the temperature of the ambient medium, $\sim$40 K where the calibrator sources reside.
   (ii) Whereas for Cas A calibrator source, currently used OFF position coordinates reside in high temperature region, $\sim$71 K as compared to the temperature of the ambient medium, $\sim$46 K where the calibrator source resides.
3) Finally, the ambient temperature of background where the north-pole resides is too low.

We hope that this document, in particular Table 4 would be useful for the Engineering team at the GMRT in order to perform appropriate system tests, thereby improve the performance of the GMRT.

## 4 References


– Haslam, C.G.T. et al., 1981 A&A, 100, 209

– Haslam, C.G.T. et al., 1982, A&AS, 47, 1

– Lal, D.V., Absolute cold sky brightness temperature of the diffuse radio background from 50 to 1500 MHz, NCRA Tech. Rep., 2014

– Lal, D.V., Flux density measurements for Cas A, Crab, Cygnus A & Virgo A calibrator sources from 50 to 1450 MHz, NCRA Tech. Rep., 2015

– Low frequency Radio Astronomy ("blue book"), Eds. J.N. Chengalur, Y. Gupta & K.S. Dwarakanath (May 2003)

– Rogers, A.E. & Bowman, J.D., 2008 AJ, 136, 641

– Sirothia, S.K., 2009 MNRAS, 398, 853


## 5 Appendix: System Parameters

Below in the Table 5, reproduced from GMRT observer's manual, we list the system parameters, including typical receiver ($T_{\rm Rx}$), ground ($T_{\rm grd}$) temperatures and antenna gain (K Jy$^{-1}$ Antenna$^{-1}$).

Table 4: Expected amount of deflection for ON–minus–OFF measurement for calibrator sources at several GMRT frequencies (upper-half) and sub-band frequencies of the $L$-band (lower-half) using methodology described in Section 2.

| | | R.A. (J2000) (hh mm ss.ss) | Dec (dd mm ss.s) | 151 | 235 | 325 | 610 | 1420 |
|---|---|---|---|---|---|---|---|---|
| | | | | Frequency (MHz) (deflection, dB) | | | | |
| Cygnus A | | | | | | | | |
| | OFF–1 | 19 18 05.89 | +47 59 23.8 | 7.04 | 9.42 | 11.42 | 10.56 | 8.22 |
| | OFF–2 | 19 06 06.33 | +31 00 00.9 | 7.02 | 9.41 | 11.41 | 10.56 | 8.22 |
| Cas A | | | | | | | | |
| | OFF–1 | 22 13 29.43 | +51 05 16.9 | 7.75 | 10.33 | 12.44 | 11.85 | 9.64 |
| | OFF–2 | 00 38 08.03 | +57 01 25.5 | 7.62 | 10.20 | 12.32 | 11.81 | 9.64 |
| Crab | | | | | | | | |
| | OFF–1 | 05 56 56.42 | +12 21 40.9 | 2.13 | 4.03 | 6.03 | 6.34 | 5.79 |
| | OFF–2 | 04 29 43.30 | +36 59 59.3 | 2.15 | 4.05 | 6.05 | 6.35 | 5.79 |
| Virgo A | | | | | | | | |
| | OFF–1 | 12 14 10.41 | +09 42 34.0 | 2.53 | 3.79 | 5.12 | 3.69 | 2.22 |
| | OFF–2 | 12 38 27.89 | +17 56 04.1 | 2.44 | 3.69 | 5.01 | 3.67 | 2.21 |

| | | R.A. (J2000) (hh mm ss.ss) | Dec (dd mm ss.s) | 1060 | 1170 | 1280 | 1390 |
|---|---|---|---|---|---|---|---|
| | | | | Frequency (MHz) (deflection, dB) | | | |
| Cygnus A | | | | | | | |
| | OFF–1 | 19 18 05.89 | +47 59 23.8 | 8.96 | 8.72 | 8.50 | 8.28 |
| | OFF–2 | 19 06 06.33 | +31 00 00.9 | 8.96 | 8.72 | 8.49 | 8.28 |
| Cas A | | | | | | | |
| | OFF–1 | 22 13 29.43 | +51 05 16.9 | 10.34 | 10.11 | 9.90 | 9.69 |
| | OFF–2 | 00 38 08.03 | +57 01 25.5 | 10.33 | 10.11 | 9.89 | 9.69 |
| Crab | | | | | | | |
| | OFF–1 | 05 56 56.42 | +12 21 40.9 | 5.93 | 5.89 | 5.85 | 5.80 |
| | OFF–2 | 04 29 43.30 | +36 59 59.3 | 5.93 | 5.89 | 5.85 | 5.80 |
| Virgo A | | | | | | | |
| | OFF–1 | 12 14 10.41 | +09 42 34.0 | 2.62 | 2.48 | 2.36 | 2.24 |
| | OFF–2 | 12 38 27.89 | +17 56 04.1 | 2.62 | 2.48 | 2.35 | 2.24 |

Table 5: Measured system parameters of the GMRT. Note: This table has been reproduced from GMRT observer's manual.

| | Frequency (MHz) | | | | |
|---|---|---|---|---|---|
| | 151 | 235 | 325 | 610 | 1420 |
| Primary beam (HPBW, arcmin) | 186 $\pm$6 | 114 $\pm$5 | 81 $\pm$4 | 43 $\pm$3 | (24 $\pm$2)$\times$(1400/$f$) |
| System temperature ($\mathrm{T}_{\mathrm{system}}$, K) | | | | | |
| Receiver temperature ($T_{\mathrm{R}}$) | 295$^{\dagger}$ | 106$^{\dagger}$ | 53 | 60 | 45 |
| Typical $T_{\mathrm{sky}}$ (off Galactic plane) | 308 | 99 | 40 | 10 | 4 |
| Typical $T_{\mathrm{grd}}$ | 12 | 32 | 13 | 32 | 24 |
| $\mathrm{T}_{\mathrm{system}}$ (= $T_{\mathrm{R}} + T_{\mathrm{sky}} + T_{\mathrm{ground}}$) | 615 | 237 | 106 | 102 | 73 |
| Antenna gain (K Jy$^{-1}$ Antenna$^{-1}$) | 0.33 | 0.33 | 0.32 | 0.32 | 0.22 |
| Synthesized beam (FWHM) | | | | | |
| – Full array (arcsec) | 20 | 13 | 9 | 5 | 2 |
| – Central square (arcsec) | 420 | 270 | 200 | 100 | 40 |
| Largest detectable structure (arcmin) | 68 | 44 | 32 | 17 | 7 |
| Usable frequency range | | | | | |
| – observatory default (MHz) | 150–156 | 236–244 | 305–345 | 580–640 | 1000–1450 |
| – allowed by electronics (MHz) | 130–190 | 230–250 | 305–360 | 570–650 | 1000–1450 |
| Fudge factor (actual to estimated time) | | | | | |
| – for short observations | 10 | 5 | 5 | 2 | 2 |
| – for long observations$^{\#}$ | 5 | 2 | 2 | 1 | 1 |
| Best RMS sensitivities achieved (mJy)$^{\ddagger}$ | 0.7 | 0.25 | 0.04 | 0.02 | 0.03 |
| Typical dynamic range achieved | $>$1500 | $>$1500 | $>$1500 | $>$2000 | $>$2000 |

† With default solar attenuator (14 dB).
# For spectral observations fudge factor is close to 1.
‡ So far known to us!